Available online at www.sciencedirect.com
ScienceDirect
Physics Letters A 372 (2008) 3484–3487
PHYSICS LETTERS A
www.elsevier.com/locate/pla

Dipole-induced, first-order phase transitions of nano-rod monolayers

Joohee Lee [a], M. Gregory Forest [a], Qi Wang [b], Ruhai Zhou [c,*]

[a] *Department of Mathematics & Institute for Advanced Materials, University of North Carolina at Chapel Hill, Chapel Hill, NC 27599-3250, USA*
[b] *Department of Mathematics, Florida State University, Tallahassee, FL 32306, USA*
[c] *Department of Mathematics and Statistics, Old Dominion University, Norfolk, VA 23529, USA*

Received 16 November 2007; accepted 10 January 2008

Available online 26 February 2008

Communicated by C.R. Doering

Abstract

The isotropic–nematic transition of nano-rod monolayers with fore–aft symmetry is second order, in stark contrast to the first-order phase transition explained by Onsager [L. Onsager, Ann. (N.Y.) Acad. Sci. 51 (1949) 627] for rods in three dimensions. Here we show that the coupling of a dipole potential to excluded volume is sufficient to re-instate a first-order phase transition of rods confined to two dimensions.

1. Introduction

In [1], Bhandar and Wiest extended the Doi–Hess–Smoluchowski equation for rigid rod nematics to dipolar nano-rod dispersions. With broken fore-aft symmetry of the rods, the possibility arises for nonzero odd moments of the orientational probability distribution function (PDF), leading to two types of ordered phases, polar–nematic and nonpolar–nematic, depending on dipole strength; the isotropic phase remains unstable above a certain volume fraction or dipole strength. Several studies have addressed three-dimensional orientational behavior of dipolar nematics using this new model [2,3,14], or its moment-closure approximations [1,4].

We focus here on the equilibrium phase diagram for monolayers of dipolar Brownian rods, where the PDF is confined to two space dimensions (2D). Maffettone and Marrucci [5] showed numerically, and the authors [6] confirmed analytically that 2D nematics with fore–aft symmetry do not share the Onsager hysteresis diagram: the isotropic–nematic transition is continuous and phases do not co-exist. Here we show the coupling of dipolar and excluded-volume potentials modifies this picture in a dramatic fashion, reinstating hysteresis and two instances of bi-stable phases whose details are described below.

2. Equilibria of coupled dipolar and excluded-volume potentials

Let $\mathbf{m}$ be a unit vector for the axis of symmetry of the rod macromolecule, and let $f(\mathbf{m},t)$ be the orientational probability distribution function (PDF) of the nano-rod ensemble. The moments of f are denoted

$$\langle \mathbf{m} \rangle = \int \mathbf{m} f(\mathbf{m},t)\, d\mathbf{m}, \tag{1}$$

$$\langle \mathbf{mm} \rangle = \int \mathbf{mm} f(\mathbf{m},t)\, d\mathbf{m}, \tag{2}$$

etc. The total potential for dipolar Brownian rods in equilibrium is given by

$$V(\mathbf{m}) = -k_B T\big[\alpha \mathbf{m}\cdot\langle \mathbf{m}\rangle + 2N\langle \mathbf{mm}\rangle : \mathbf{mm}\big], \tag{3}$$

where α measures the dipole strength, and N is the normalized strength of the Maier–Saupe excluded-volume potential.

The rotational transport equation for the PDF is the extended Doi–Hess–Smoluchowski equation [1,7,8]

$$\frac{\partial}{\partial t} f = D_r^0 \frac{\partial}{\partial \mathbf{m}} \cdot \left(f \frac{\partial \mu}{\partial \mathbf{m}} \right), \tag{4}$$

$$\mu = \ln f + \frac{1}{k_B T} V, \tag{5}$$

* Corresponding author.
E-mail address: rzhou@odu.edu (R. Zhou).

0375-9601/$ – see front matter
doi:10.1016/j.physleta.2008.01.087

where $\frac{\partial}{\partial \mathbf{m}} = (\mathbf{I} - \mathbf{mm}) \cdot \nabla$ is the rotational gradient operator, D_r^0 is an averaged relaxation rate, a is a particle shape parameter related to the rod aspect ratio r as $a = \frac{r^2-1}{r^2+1}$, and μ is the normalized chemical potential. Steady states of (4) are of Boltzmann type,

$$f = \frac{1}{Z} e^{-\frac{1}{k_B T} V}, \tag{6}$$

where Z is the normalizing coefficient. We now follow recent analysis of Boltzmann distributions of Constantin et al. [9] and extensions in [2,3]. Step 1 is to rigorously reduce the infinite-dimensional nonlinear diffusion equation (4) to a finite-dimensional (here 2) system of nonlinear integral equations. Then Step 2 is to use parameter continuation software AUTO [10] to solve the equilibrium equations across the parameter space of dipolar and excluded volume strength. Finally, we determine stability by convexity of the free energy at the equilibria in question. The results are captured by Fig. 1, which we now explain.

Let $\mathbf{n}_1, \mathbf{n}_2$ be the two orthonormal eigenvectors of the second moment tensor $\langle \mathbf{mm} \rangle$. Then

$$\begin{aligned} \langle \mathbf{m} \rangle &= s_1 [\cos\theta' \mathbf{n}_1 + \sin\theta' \mathbf{n}_2], \\ \langle \mathbf{mm} \rangle &= s \left(\mathbf{n}_1 \mathbf{n}_1 - \frac{1}{2} \mathbf{I} \right) + \frac{1}{2} \mathbf{I}, \end{aligned} \tag{7}$$

where s_1 is a *polar order parameter* which measures the average polarity in the dispersion.

For equilibria of (4), the first moment of f is in the eigenspace of the second moment [2,11], so we choose $\langle \mathbf{m} \rangle$ parallel to $\mathbf{n}_1$. By the methods of [9] equilibria are uniquely specified by the first two moments, which are further invariant under rotations, so the PDF is uniquely specified by the order parameters s_1 and s. Equilibrium solutions of the PDE (4) are thereby reduced to two nonlinear integral equations for s_1 and s:

$$\int_0^{2\pi} (s_1 - \cos\theta) e^{\alpha s_1 \cos\theta + N s \cos 2\theta} \, d\theta = 0, \tag{8}$$

$$\int_0^{2\pi} (s - \cos 2\theta) e^{\alpha s_1 \cos\theta + N s \cos 2\theta} \, d\theta = 0. \tag{9}$$

For any α and N, the class of nonpolar solutions with $s_1 = 0$ always exist, corresponding to the previously studied isotropic–nematic solutions with fore-aft symmetry.

First we solve the equilibrium integral equations (8), (9) using the continuation software AUTO [10]. Then stability is determined by examining convexity of the free energy density:

$$A[f] = \int_{\|\mathbf{m}\|=1} \left[k_B T \ln f + \frac{V}{2} \right] f \, d\mathbf{m}. \tag{10}$$

Equilibria are classified in terms of s_1 and s: $s_1 > 0$ implies a polar phase (non-zero first moment), and $s > 0$ implies a nematic phase (anisotropic second moment). States with $s_1 = s = 0$ are isotropic (**I**), while states with $s_1 > 0$ and $s = 0$ do not exist. Anisotropic states satisfying: $s_1 = 0$, $s > 0$ are called nematic–nonpolar (**N–NP**); $s_1 > 0$, $s > 0$ are called nematic–polar (**N–P**). The phase diagram of stable equilibria vs dipolar strength α and excluded volume strength N is given in Table 1, where stable (unstable) phases are labeled by an "s" ("u") superscript.

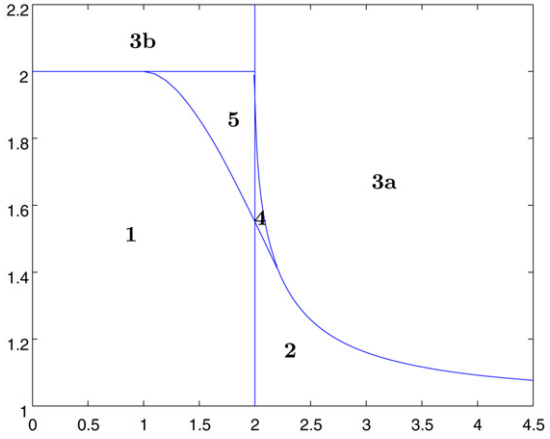

Fig. 1. Equilibrium phase diagram for Brownian rods dispersions. N and α parameterize strengths of the excluded-volume and dipolar potentials, respectively.

Table 1
With reference to the equilibrium phase diagram of Fig. 1, a catalog of all coexisting equilibria in each regions 1–5, both stable (superscript s) and unstable (superscript u). Regions 4 and 5 possess bi-stable phases

Region	Type of solutions
1	$\mathbf{I}^{\mathrm{s}}$
2	$\mathbf{I}^{\mathrm{u}}$, $\mathbf{N–NP}^{\mathrm{s}}$
3a	$\mathbf{I}^{\mathrm{u}}$, $\mathbf{N–NP}^{\mathrm{u}}$, $\mathbf{N–P}^{\mathrm{s}}$
3b	$\mathbf{I}^{\mathrm{u}}$, $\mathbf{N–P}^{\mathrm{s}}$
4	$\mathbf{I}^{\mathrm{u}}$, $\mathbf{N–NP}^{\mathrm{s}}$, $\mathbf{N–P}^{\mathrm{s}}$, $\mathbf{N–P}^{\mathrm{u}}$
5	$\mathbf{I}^{\mathrm{s}}$, $\mathbf{N–P}^{\mathrm{s}}$, $\mathbf{N–P}^{\mathrm{u}}$

The set of stable solutions divides the domain into 5 regions, distinguished by the distinct type and number of stable phases. Table 1 gives the collection of stable *and* unstable equilibria. The boundaries between regions 1–5 correspond to phase transitions, where either the number or stability of equilibria change.

The new phenomena arise in regions 4 and 5. Region 5 is the analog of three-dimensional Onsager-like, bi-stable isotropic and polar nematic phases, whereas region 4 corresponds to bi-stable nematic phases, one polar and another nonpolar.

Regions 1 and 2, where the dipolar strength is low, correspond to persistence of the nonpolar phase diagram of Maffettone et al. [12] and the authors [6], where s_1 is always zero. In region 3, the only stable phase is polar-nematic $s_1 > 0$, $s > 0$.

3. Onsager-like monolayer equilibrium phase diagrams

For different $\alpha = \text{const}$ slices, Figs. 2, 3, phase transitions (where loss or gain of stable phases occur) are recognized and classified in terms of specific bifurcations. In the dynamical systems literature, these are called "bifurcation diagrams". The

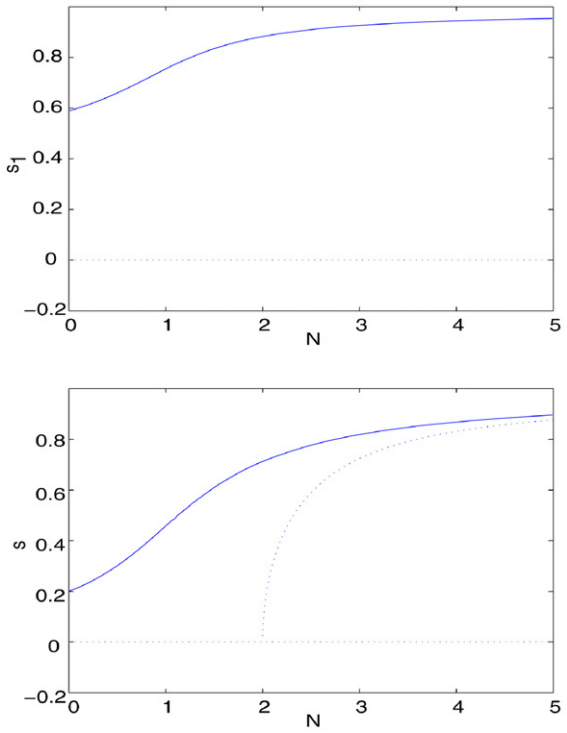

Fig. 2. Branches of equilibria, characterized by polar (s_1) and nematic (s) order parameters, versus excluded-volume potential strength N for a relatively strong dipolar potential strength $\alpha = 2.5$. Solid (dashed) curves denote stable (unstable) equilibria. Three distinct branches of equilibria (s_1, s) arise: a stable nematic–polar (**N–P**) phase $(s_1 > 0, s > 0)$ for all N; an unstable isotropic **I** phase $(s_1 = s = 0)$ for all N; and an unstable nematic–nonpolar (**N–NP**) branch $(s_1 = 0, s > 0)$ for $N > 2$.

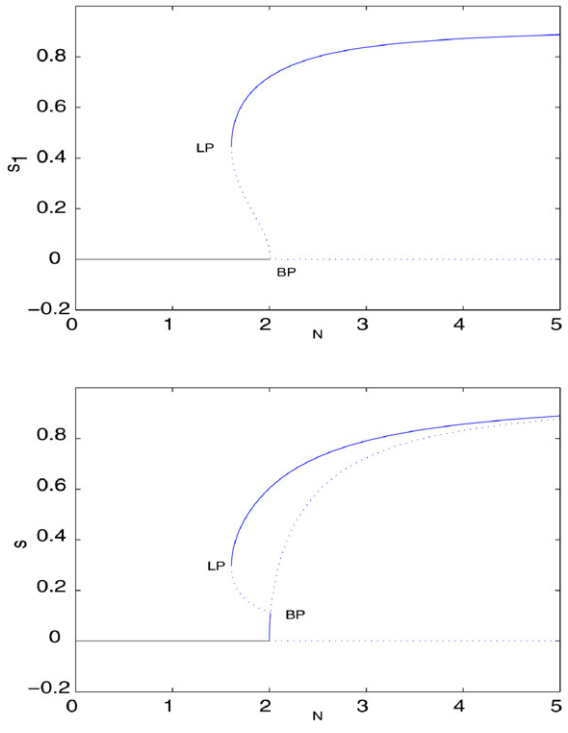

Fig. 3. Branches of equilibria, characterized by polar (s_1) and nematic (s) order parameters, versus excluded-volume potential strength N for a moderate dipolar potential strength, $\alpha = 1.8$. Solid (dashed) curves denote stable (unstable) equilibria. In addition to the isotropic–nematic transition at $N = 2$, two bifurcations (phase transitions) are identified: at $N = 2.01$ (labeled BP), where a new polar–nematic branch emerges from the purely nematic branch; and at $N = 1.61$ (labeled LP), which is a turning point of the **N–P** branch.

point bifurcations (BP, LP) in Fig. 3 correspond to the intersection of $\alpha = \text{const}$ lines with the boundaries between Regions in 1. BP is a turning point bifurcation (on one side the equilibria no longer exist, on the other side stable and unstable branches co-exist), while LP is a standard instability bifurcation where a branch of equilibria transitions from stable to unstable.

Fig. 2 is the bifurcation diagram for $\alpha = 2.5$, which is above the critical dipolar strength $\alpha = 2$. Isotropic and purely nematic branches exist, but they are unstable, yielding to a unique stable polar–nematic equilibrium for all N. Thus, a sufficiently strong dipolar potential always yields an ordered polar–nematic phase, and there are no phase transitions versus concentration for strongly dipolar rod dispersions.

Fig. 3 is the bifurcation diagram for $\alpha = 1.8$. The stable nematic branch arises at $N = 2$ as a nonpolar ($s_1 = 0$) equilibrium, but then soon thereafter becomes unstable at $N_c = 2.01$. The nonpolar–nematic branch is stable only in a narrow range between $N = 2$ and $N_c = 2.01$, corresponding in Fig. 1 to region 4. For N just past N_c, there is a first-order phase transition to a stable polar–nematic branch. If one then lowers N while on the polar–nematic branch, it persists all the way down to $N_t = 1.61$, which is a turning point bifurcation below which the phase does not exist. Thus the classical Onsager hysteresis diagram is recovered! Bi-stable isotropic and polar–nematic phases exist between $N = 1.61$ and $N = 2$, while bi-stable nematic–polar and nematic–nonpolar phases exist between $N = 2$ and $N_c = 2.01$. Below $N = 1.61$, the unique stable phase is isotropic, and above $N_c = 2.01$, the unique stable phase is polar–nematic.

4. Conclusion

We have rigorously characterized all equilibria of dipolar Brownian rod monolayers with excluded-volume interactions in terms of classical Boltzmann distributions, following Onsager [13] and Constantin et al. [9]. The salient physical phenomenon is the recovery of bi-stable phases and hysteresis in monolayers due to broken fore-aft symmetry of the rods, which are completely suppressed in monolayers of nonpolar Brownian rods.

References

[1] A.S. Bhandar, J.M. Wiest, J. Colloid Interface Sci. 257 (2003) 371.
[2] G. Ji, Q. Wang, P. Zhang, H. Zhou, Commun. Math. Sci. 5 (2008) 917.
[3] Q. Wang, S. Sircar, H. Zhou, Commun. Math. Sci. 3 (2005) 605.
[4] S. Grandner, S. Heidenreich, P. Ilg, S. Klapp, S. Hess, Phys. Rev. Lett., in press.
[5] G. Marrucci, P.L. Maffettone, Macromolecules 22 (1989) 4076.
[6] J. Lee, M.G. Forest, R. Zhou, Discrete Continuous Dynam. Syst. Ser. B 6 (2006) 339.
[7] M. Doi, J. Polym. Sci. 19 (1981) 229.
[8] S. Hess, Z. Naturforsch. A 31 (1976) 1034.

[9] P. Constantin, I. Kevrekidis, E.S. Titi, Discrete Continuous Dynam. Syst. 11 (2004) 101.
[10] E.J. Doedel, et al., Manuscript, Concordia University, 1998.
[11] J. Lee, Ph.D. Dissertation, University of North Carolina, 2007.
[12] P.L. Maffettone, S. Crescitelli, J. Non-Newtonian Fluid Mech. 59 (1995) 73.
[13] L. Onsager, Ann. (N.Y.) Acad. Sci. 51 (1949) 627.
[14] M.G. Forest, S. Sircar, Q. Wang, R. Zhou, Phys. Fluids 18 (2006) 103102.